

## Comparison of different models for computation of light distribution inside photobioreactors

C. McHardy<sup>1</sup>, G. Luzi<sup>2</sup>, J. R. Agudo<sup>2</sup>, C. Rauh<sup>1,2,3</sup>, A. Delgado<sup>1,3</sup>

<sup>1</sup>Department of Food Biotechnology and Food Process Engineering, Technische Universität Berlin, D-14195 Berlin, Germany

<sup>2</sup>Institute of Fluid Mechanics, FAU Busan Campus, University of Erlangen-Nuremberg, 618-230 Busan, Republic of Korea

<sup>3</sup>Institute of Fluid Mechanics, University of Erlangen-Nuremberg, D-91058 Erlangen, Germany

Bubble column bio-reactors, Light distribution, Lattice Boltzmann, Numerical simulations

### Abstract

Microalgae are regarded as a potential choice for a sustainable production of food, feed or fuels. The cultivation of these microorganisms occurs in photobioreactors (PBR), where light distribution is a key aspect for their growth and it is a crucial parameter for the reactor productivity. Besides, it is the primary energy source for the cellular metabolism of phototrophs. The Radiative Transfer Equation (RTE) governs the light propagation in turbid media, whose optical properties change spatially due to the local variation of the air volume fraction. Nevertheless, the influence of the gas phase on the light attenuation is scarcely considered in literature.

In the present contribution, we first simulate the fluid flow in a bubble column PBR, and then we utilise the spatial distributions of the gaseous and the liquid phase to compute the spectral radiation characteristics of microalgae suspensions. Subsequently, we simulate the light field by means of a recently developed lattice Boltzmann solver, and then we compare the results with simpler models available in literature.

### Introduction

Microalgae are commonly cultivated in closed PBR and they use the energy of light to convert carbon dioxide into biomass. The light distribution inside PBR is a decisive parameter for the photosynthesis (Williams and Laurens., 2010), and it is strongly affected by the presence of microorganisms. Since they absorb and scatter light, they attenuate light intensity. Moreover, anisotropic scattering makes an accurate prediction of local light intensities a challenging task, first because the scattering characteristics of the microorganisms need to be measured (Kandilian et al., 2016), and second because an accurate computation of light distribution by scattering requires an adequate discretization of scattering kernel of the RTE (Hunter and Guo, 2015). Therefore, in the course of computing light distributions, scattering effects are often simplified. Most consistently, this is done in the Lambert Beer law, where scattering is fully neglected. Other models, like so-called Cornets model (Pottier et al. 2005) assume light propagation to be a quasi 1D problem, which simplifies the computation significantly and enables analytical solutions.

Another simplification is that a homogeneous cell distribution is commonly assumed inside PBR. However, most of PBR are aerated in order to furnish carbon dioxide to the suspension, obtain an adequate mixing of the liquid phase and remove oxygen (Olivieri et al., 2014). The presence of gas modifies the local scattering characteristics of a suspension, being those of bubbles different than those of microalgae cells. Therefore, the hydrodynamic characterization of a PBR is necessary, and it can be predicted with the aid of Computational Fluid Dynamics (CFD). Since two-dimensional simulations may produce unrealistic results (Mudde et al., 1996), and they may exhibit a strong grid dependency (Bech 2005), fully three dimensional unsteady computations are required. They are able to predict, at least qualitatively, the typical complex flow patterns of a bubble column PBR (Pfleger et al., 1999, Masood and Delgado, 2014). CFD can also be combined with numerical simulations of light distribution and kinetic growth. Simple approaches opt for the Lambert Beer law and the Aiba model (Zhang et al., 2015), while more sophisticated ones make use of ray tracing simulations and an empirical three-parametric equation (Krujatz et al. 2015). Other researchers integrate a compartmental with a photosynthetic factory model (Nahua et al., 2013), including also light directionality and day and night time conditions (Nahua et al., 2015). In the present contribution, we first simulate numerically the bubble column flow inside a cylindrical PBR. Afterwards, we compute the radiation characteristics of the suspension by weighting the radiation characteristics of gas bubbles and those of microorganisms. Finally, we compare the numerical solution of the RTE, obtained with a lattice Boltzmann solver (McHardy et al., 2016), with simpler analytical models.

### Simulation set-up: CFD

#### *Geometry and mesh*

The PBR has a cylindrical shape with a small inlet located in one base. The diameter of the PBR is 5 [cm] and its height is 50 [cm]. The diameter of the inlet sparger is 1 [cm]. Both the geometry and the mesh have been generated with the aid of the commercial software ANSYS ICEM<sup>®</sup>. We cover our domain with a structured grid of 54802 volumes, see Fig. 1. The mesh has been refined near the walls and it is equally spaced along the axial direction.

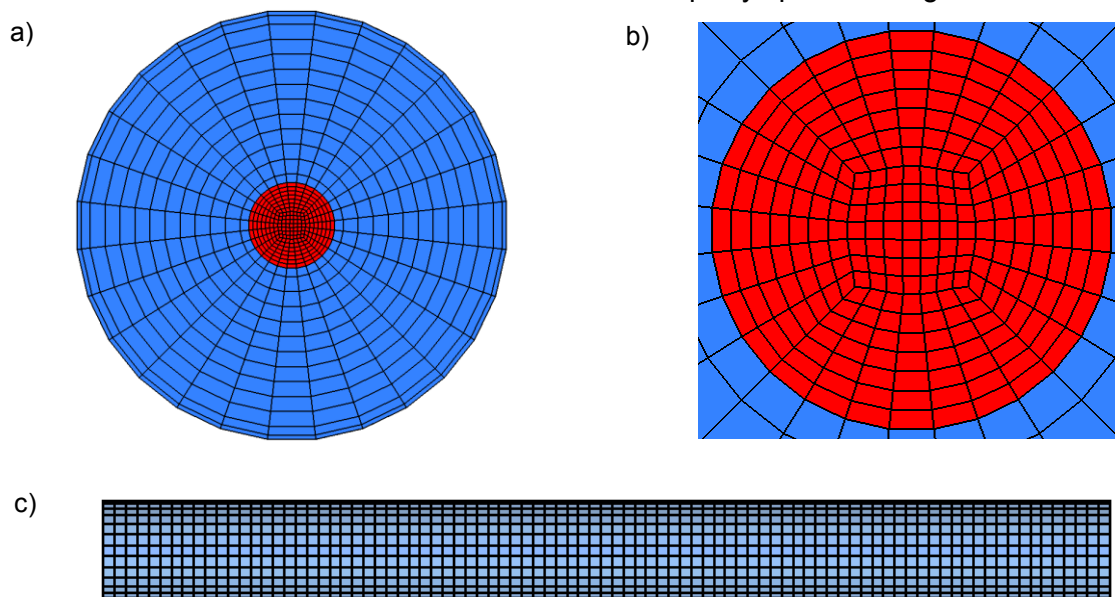


Fig. 1 a) meshed base of the cylinder containing the inlet, b) focus on the meshed inlet sparger, c) side view (light blue to highlight the grid) of the PBR.

### Mathematical modelling of fluid flow

The Eulerian formulation of the Reynolds averaged form of the mass conservation equation for each phase may be written as

$$\frac{\partial}{\partial t}(\rho_k \alpha_k) + \nabla \cdot (\rho_k \alpha_k \mathbf{u}_k) = 0 \quad (1)$$

where  $\rho_k$ ,  $\alpha_k$  and  $\mathbf{u}_k$  are the density, volume fraction and velocity of each phase. The subscript  $k$  indicates the phase:  $L$  stands for the liquid and  $G$  for the gas phase. The momentum equations for multiphase flows read

$$\frac{\partial}{\partial t}(\rho_k \alpha_k \mathbf{u}_k) + \nabla \cdot (\rho_k \alpha_k \mathbf{u}_k \mathbf{u}_k) = \nabla \cdot (\alpha_k \boldsymbol{\tau}_k) - \alpha_k \nabla p + \rho_k \alpha_k \mathbf{g} + \mathbf{M}_{s,k} \quad (2)$$

where,  $s = L, G$ . The left-hand side of Eq. 2 contain the temporal and the convective acceleration of each phase, while the right-hand side contain the divergence of the viscous stress tensor, pressure gradient, gravity and interphase momentum forces (Pfleger et al. 1999). The stress tensor is

$$\boldsymbol{\tau}_k = \mu_{k,eff} \left[ \nabla \mathbf{u}_k + (\nabla \mathbf{u}_k)^T - \frac{2}{3} \mathbf{I}(\nabla \cdot \mathbf{u}_k) \right] \quad (3)$$

where the effective viscosity  $\mu_{k,eff}$  is the sum of the molecular and the turbulent viscosity

$$\mu_{k,eff} = \mu_{k,Lam} + \mu_{k,Turb} \quad (4)$$

The last term of the right-hand side of Eq. (2) represents the interphase momentum forces,  $\mathbf{M}_{s,k}$ . In our simulations, we consider the drag, lift, virtual mass, wall lubrication and dispersion forces. We compute the drag coefficient  $C_D$  with the Grace correlation (Grace et al., 1976), the lift coefficient  $C_L$  with the Legendre-Magnaudet model (Legendre et al., 1998) and the wall lubrication force coefficient  $C_{WL}$  with the Frank model (Frank et al., 2004; Frank et al., 2008). We retain the virtual mass coefficient  $C_{VM} = 0.5$ , and we employ the Favre averaged model (Burns et al., 2004) for the turbulent dispersion forces. In order to compute the turbulent eddy viscosity  $\mu_{k,Turb}$  of each fluid, we choose the Shear Stress Transport (SST) model (Menter 1999) for the water and the dispersed phase zero equation for the air.

### Radiation characteristics of the suspension

In order to compute the radiative properties of a mixture, we superimpose the radiation characteristics of single components (Pilon et al., 2011), i.e.

$$\kappa(\mathbf{x}) = \kappa_A (1 - \alpha_G(\mathbf{x})) \quad (5a)$$

$$\sigma(\mathbf{x}) = \sigma_A (1 - \alpha_G(\mathbf{x})) + \sigma_B \quad (5b)$$

where  $\kappa$  and  $\sigma$  are the effective absorption and scattering coefficients, while  $\kappa_A$  and  $\sigma_A$  are the those of the suspension. They are related to the mass concentration  $c_A$ , the absorption and scattering cross-sections  $A_{ABS}$  and  $A_{SCA}$  via the relations

$$\kappa_A = c_A A_{ABS} \quad (6a)$$

$$\sigma_A = c_A A_{SCA} \quad (6b)$$

This assumption is valid in the single-digit gram-per-liter range, typical for PBR. In case of gas bubbles, we only consider scattering effects, being the adsorption ones negligible compared to those of microalgae. Therefore, for bubbles we have

$$\kappa_B = 0 \quad (7a)$$

$$\sigma_B(x) = \alpha_G(x) \frac{A_B Q_{sca}}{V_B} \quad (7b)$$

where  $V_B$  is the volume,  $A_B$  is the geometrical cross-section of a single bubble and  $Q_{sca}$  the scattering efficiency. Finally, we use an effective scattering phase function weighted with the volumetric scattering coefficients of both microalgae and gas bubbles, i.e.

$$\Phi(x) = \frac{(1 - \alpha_G(x)) \sigma_A \Phi_A + \sigma_B \Phi_B}{(1 - \alpha_G(x)) \sigma_A + \sigma_B} \quad (8)$$

### *Mathematical modelling of light distribution: the RTE*

The light propagation in turbid media is governed by the RTE, which may be written as

$$\frac{1}{c} \frac{\partial}{\partial t} I(x, \hat{s}, t) + \hat{s} \cdot \nabla I(x, \hat{s}, t) = \beta \left( -I(x, \hat{s}, t) + \frac{\omega}{4\pi} \int_{4\pi} I(x, \hat{s}', t) \Phi(\hat{s}', \hat{s}) d\Omega \right) \quad (9)$$

where  $I(x, \hat{s}, t)$  is the radiation intensity,  $c$ ,  $t$ ,  $\Omega$ ,  $\beta$ ,  $\hat{s}$  and  $x$  denote speed of light, time, solid angle, extinction coefficient, unit direction and position vector. The scattering albedo  $\omega$  is defined as

$$\omega = \frac{\sigma}{\sigma + \kappa} \quad (10)$$

The extinction coefficient is the sum of the effective adsorption and scattering coefficients, i.e.  $\beta = \kappa + \sigma$ , that have been defined in Eqs. (5a) and (5b), respectively. Additionally, in Eq. (9)  $\Phi$  is the scattering phase function, which models the angular distribution of scattered light. We solve Eq. (9) by means of a lattice Boltzmann method developed by (McHardy et al., 2016). Details of the discretized form and the numerical solution of Eq. (9) are given in (McHardy et al., 2016, McHardy et al., 2017) and will not be repeated here.

### *Mathematical modelling of light distribution: analytical expressions*

Lambert Beer's law is the analytical solution of a 1D simplification of Eq. (9) which fully neglects the effects of scattering. The analytical expression reads

$$I(x + \Delta x) = I(x) \exp(-\kappa(x) \Delta x) \quad (11)$$

The second model we test is Cornet's model (Pottier et al. 2005), which is based on the Schuster-Schwarzschild Two-Flux approximation of Eq. (9). For collimated light and non-reflecting boundaries it reads

$$\frac{I(x)}{I_0} = \frac{-(1 - \alpha) \exp(-\delta L) \exp(\delta x) + (1 + \alpha) \exp(\delta L) \exp(-\delta x)}{(1 + \alpha)^2 \exp(\delta L) - (1 - \alpha)^2 \exp(-\delta x)} \quad (12)$$

where  $\alpha = \sqrt{\kappa / (\kappa + 2b\sigma)}$ ,  $\delta = \sqrt{\kappa(\kappa + 2b\sigma)}$ . For Henyey-Greenstein phase functions, the backscattering fraction  $b$  is given as

$$b = \frac{1-g}{2g} \left[ \frac{1+g}{\sqrt{1+g^2}} - 1 \right] \quad (13)$$

where  $g$  is the anisotropy factor. The original version of Cornets model (Cornet et al. 1994) assumes isotropic scattering and uses the reduced scattering coefficient  $\sigma'_A = \sigma_A(1-g)$  instead of  $\sigma_A$ . The model equation reads

$$\frac{I(x)}{I_0} = \frac{(1+\alpha)\exp(-\delta(x/L-1)) - (1-\alpha)\exp(\delta(x/L-1))}{(1+\alpha)^2\exp(\delta L) - (1-\alpha)^2\exp(-\delta x)} \quad (14)$$

It is important to state that Eqs. (12) and (14) can only be applied to optical homogeneous media, that is,  $\kappa, \sigma, g, b = const$ .

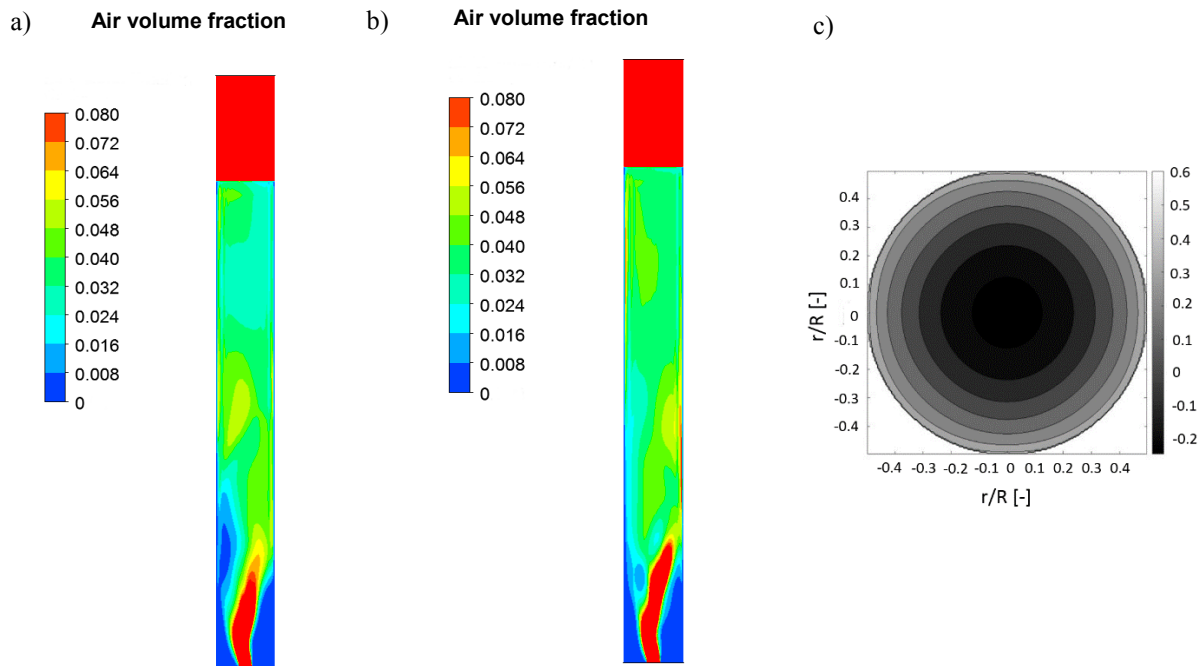
### Simulation details

We perform all the numerical simulations of fluid flow by means of the commercial software ANSYS CFX<sup>®</sup>, which is a node-centred finite volume solver. At the inlet, we specify an air mass flow rate and we set the outlet as an opening boundary condition. The other surfaces of the geometry have been set as walls, with a no-slip boundary condition for both fluids. Additionally, we leave an air headspace in the last 10 [cm] of the reactor. Furthermore, we set a constant fixed mean bubble diameter,  $d_B = 7$  [mm]. We ran unsteady simulations with a value of gas superficial velocity of  $U_G = 8.5$  [mm/s]. We choose a variable adaptive time step, whose maximum value is  $\Delta t = 1.25 \cdot 10^{-3}$  [s], and its minimum one is  $\Delta t = 5 \cdot 10^{-4}$  [s]. The time step decrease and increase factors are 0.5 and 2, respectively. The maximum number of inner iterations is thirty and the convergence criteria are met when the scaled residuals of velocity and pressure are below the value of  $10^{-4}$ .

The different models for computations of light distributions have been implemented in Matlab 2016b<sup>®</sup>. For the lattice Boltzmann method, we make use of a structured lattice with approximately  $1E07$  nodes, while we evaluate analytical models at similar distances. Moreover, we assume that the reactor is illuminated from four sides by plane light sources, emitting directed light. Reflections and refraction caused by the curved boundaries of the reactor have been neglected. Radiation characteristics of an optically inhomogeneous medium have been computed according to Eqs. (5-8), while for optically homogeneous media Eq. (6) has been applied. The radiation characteristics of microalgae have been assumed to be equal to those measured by Kandilian et al. (2016) for *C. reinhardtii*. We utilize the anisotropy factors  $g_A = 0.97$  for cells and  $g_B = 0.86$  for bubbles.

### Results and discussion

A typical characteristic of an aerated bioreactor flow is a meandering air bubble “plume”, see Fig. 2 a), and Fig. 2b), at two different time instants. The chaotic movement of the bubble plume generates three-dimensional vortical structures in the liquid phase that dominate the bubble column hydrodynamics. Figure 2 c) shows the dimensionless logarithmic light intensity as predicted by Cornets model, Eq. (12). It can be seen that for optically homogeneous media directed illumination from four sides results in a profile of light intensity which is symmetric in the azimuthal direction. Qualitatively, similar patterns can be observed for all of the considered models in optically homogeneous media.



Air volume fraction on an x-y plane at  $z=0$  at Fig. 2a)  $t=129.45$  [s], Fig. 2b)  $t=135.7$  [s]. The gas superficial velocity is  $8.5$  [mm/s], Fig. 2c) Logarithmic dimensionless intensity  $\log I/I_0$  in the x-z plane as predicted by Cornets model, Eq. (12), for an optically homogeneous medium with biomass concentration of  $1 \text{ kg/m}^3$  and wavelength of  $700 \text{ nm}$ .

### Prediction of different light propagation models

Fig. 3 shows the profiles of light intensity at  $\lambda = 520 \text{ nm}$  and  $\lambda = 655 \text{ nm}$  as predicted by different models, for a biomass concentration  $c_A = 0.5 \text{ kg/m}^3$ . At  $\lambda = 520 \text{ nm}$  the absorption is relatively weak while at  $\lambda = 655 \text{ nm}$ , it is close to the absorption maximum of microalgal pigments. It can be seen that the original isotropic Cornet model, Eq. (14), always predicts the highest attenuation. In contrast, compared to the other analytical models, the Lambert-Beers law predicts the lowest attenuation. This occurs since backscattering effects are neglected. The effect of spatially inhomogeneous radiation characteristics, due to the presence of bubbles, is negligible and averaged profiles of the RTE are almost symmetric. However, the air reduces the absorption coefficient which results in lower attenuation, in case of the inhomogeneous Lambert-Beers law as compared to the homogeneous one. Fig. 4 depicts the results of the analytical models compared to the averaged intensity profiles computed solving the RTE. For the analytical models, the homogeneous radiation characteristics have been computed by Eqs. (5)-(8), assuming an averaged air volume fraction in the whole PBR. For low biomass concentrations the light intensity profiles of the RTE, anisotropic Cornet model and Lambert-Beer's law show minimal deviations, while again the isotropic Cornet model predicts the highest attenuation. In case of higher biomass concentrations, the effects of scattering lead to higher deviations between the models.

### Discussion

Analytical models have been used to compute the light distribution in inhomogeneous microalgae suspensions. If the presence of air is considered in the calculation of radiation characteristics, the predicted light intensity profiles match quantitatively those computed numerically. Computations of air volume fractions by means of CFD provide the required information in order to compute the effective radiation characteristics. However, analytical solutions of light propagation models are restricted to simple geometries, and limitations can occur if complex

geometries and boundary effects must be considered. In such situations, the full 3D solution of the RTE is required. Our results indicate that accurate solutions of the RTE can be also be obtained using averaged radiation characteristics, since local effects does not to affect strongly the light intensity profiles, at least under the conditions we investigated in this work. This is a beneficial result, since spatial inhomogeneity cause a much higher computational cost compared to the case of an optically homogenous media. However, our findings need further investigations, since the considered parameter space captures just a small portion of the possible conditions of a PBR.

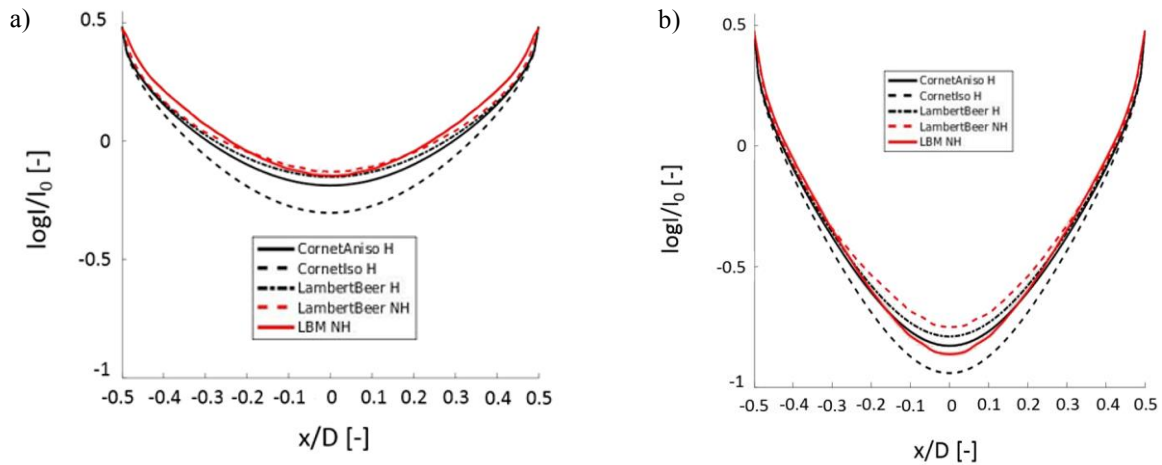


Fig. 3 Predictions of light intensity profiles inside a PBR according to different models for two wavelengths. Black lines denote the solutions of analytical models. Red lines are the solutions of the Lambert-Beers law and the RTE (computed with LBM), taking into account the presence of gas bubbles. The profile of the numerical solution of the RTE is averaged over the reactor height: a) 520 nm, b) 655 nm.

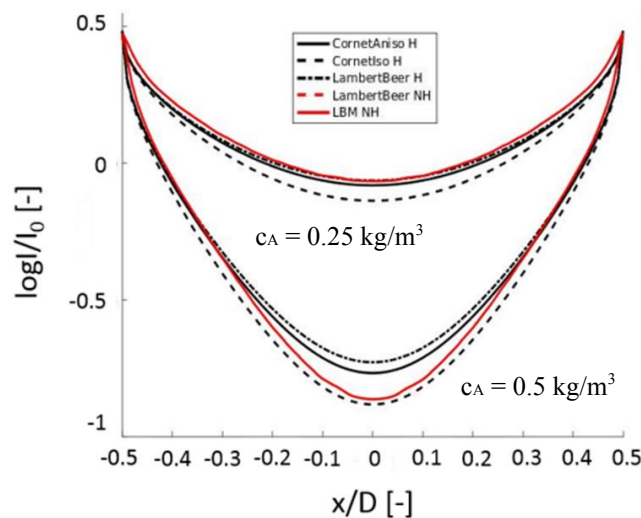


Fig. 4 Predictions of different models with radiation characteristics considering an averaged air volume fraction. The solution of the RTE is computed by using inhomogeneous radiation characteristics.

## Literature

- Bech, K., 2005:** "Dynamic simulation of a 2D bubble column", *Chem. Ing. Sci.*, 60(19), pp. 5294-5304
- Burns, A. D. B., Frank, Th., Hamill, I., Shi, J-M., 2004:** "The Favre Averaged Drag Model for Turbulent Dispersion in Eulerian Multi-Phase Flows", 5th International Conference on Multiphase Flow
- Cornet, J.F., Dussap, C.G., Gros, J.B. 1994:** "Conversion of radiant light energy in photobioreactors", *AIChE Journal*, 40(6), pp.1055-1066
- Frank, Th., Shi, J. M., Burns, A. D., 2004:** "Validation of Eulerian Multiphase Flow Models for Nuclear Safety Applications", 3rd International Symposium on Two-Phase Flow Modelling and Experimentation, Pisa, Italy
- Frank, Th., Zwart, P. J., Krepper, E., Prasser, H.-M., Lucas, D., 2008:** "Validation of CFD models for mono- and polydisperse air-water two-phase flows in pipes", *J. Nuclear Engineering & Design*, 238(3), pp. 647–659
- Grace, J. R., Wairegi, T., Nguyen, T. H., 1976:** "Shapes and velocities of single drops and bubbles moving freely through immiscible liquids", *Trans. Inst. Chem. Eng.*, 54 (3), pp. 167-173
- Hunter, B., Guo, Z., 2015:** "Numerical smearing, ray effect, and angular false scattering in radiation transfer computation", *Int. J. Heat Mass Transfer*, 81, pp. 63–74
- Kandilian, R., Pruvost, J., Artu, A., Lemasson, C., Legrand, J., Pilon, L., 2016:** "Comparison of experimentally and theoretically determined radiation characteristics of photosynthetic microorganisms", *J. Quant. Spectrosc. Ra.*, 175, pp. 30-54
- Krujatz, F., Illing, R., Krautwer, T., Liao, J., Helbig K., Goy, K., Opitz, J., Cuniberti, G., Bley, T., Weber, J., 2015:** "Light-field-characterization in a continuous hydrogen-producing photobioreactor by optical simulation and computational fluid dynamics", *Biotechnol Bioeng.*, 112(12), pp. 2439-2449
- Legendre, D., Magnaudet, J., 1998:** "The lift force on a spherical bubble in a viscous linear shear flow", *J. Fluid Mech.*, 368, pp. 81-126
- Masood, R. M. A., Delgado A. 2014:** "Numerical investigation of the interphase forces and turbulence closure in 3D square bubble columns", *Chem. Eng. Sci.*, 108, pp.154-168
- McHardy, C., Horneber, T., Rauh, C., 2016:** "New lattice Boltzmann method for the simulation of three-dimensional radiation transfer in turbid media", *Opt. Express*, 24(15), pp. 16999-17017
- McHardy, C., Horneber, T., Rauh, C., 2017:** "Spectral Simulation of Light Propagation by using a lattice Boltzmann method for Photons", *Appl. Math. Comput.*(in press)
- Menter, F. R., 1994:** "Two-equation eddy-viscosity turbulence models for engineering applications", *AIAA Journal*, 32(8), pp. 1598-1605
- Mudde, R.F., Simonin, O., 1999:** "Two- and three-dimensional simulations of a bubble plume using a two-fluid model", *Chem. Eng. Sci.*, 54, pp. 5061-5069
- Nauha, E. K., Alopaeus, V. 2013:** "Modeling method for combining fluid dynamic and algal growth in a bubble column photobioreactor", *Chem. Eng. Journal*, 229, pp. 559-568
- Nauha, E. K., Alopaeus, V. 2015:** "Modeling outdoors algal cultivation with compartmental approach", *Chem. Eng. Journal*, 259, pp. 945-960
- Olivieri, G., Salatino, P., Marzocchella, A., 2014:** "Advances in photobioreactors for intensive microalgal production: configurations, operating strategies and applications", *J. Chem. Technol. Biotechnol.*, 89, pp. 178-195
- Pilon, L., Berberoglu, H., Kandilian, R., 2011:** "Radiation transfer in photobiological carbon dioxide fixation and fuel production by microalgae", *J. Quant. Spectrosc. Ra.*, 112(17), pp. 2639-2660
- Pfleger D., Becker S. 2001:** "Modelling and simulation of the dynamic flow behavior in a bubble column", *Chem. Eng. Sci.*, 56, pp. 569-582
- Pottier, L., Pruvost, J., Deremetz J, Cornet J.F., Legrand J., Dussap C.G., 2005:** "A fully predictive model for one-dimensional light attenuation by *Chlamydomonas reinhardtii* in a torus photobioreactor", *Biotechnol Bioeng.*, 91(5), pp. 2439-2449
- Williams, P. J. le B., Laurens, L. M. L., 2010:** "Microalgae as biodiesel & biomass feedstocks: Review & analysis of the biochemistry, energetics & economics", *Energy Environ. Sci.*, 3(5), pp. 554-590
- Zhang, D., Dechatiwongse, P., Hellgardt, K., 2015:** "Modeling light transmission, cyanobacterial growth kinetics and fluid dynamics in a laboratory scale multiphase phot-bioreactor for biological hydrogen production", *Algal Research* 8, pp. 99-107